Modeling Retina Adaptation with Multiobjective Parameter Fitting

Pablo Martínez-Cañada(✉), Christian Morillas, Samuel Romero, and Francisco Pelayo

CITIC and Department of Computer Architecture and Technology, University of Granada, Granada, Spain
{pablomc,cmg,sromero,fpelayo}@ugr.es

Abstract. The retina continually adapts its kinetics, average response and sensitivity to the conditions of the environment. Retinal neurons adapt essentially to the mean light intensity and its temporal fluctuations over the mean, also called temporal contrast. Contrast adaptation has two distinct temporal expressions with fast and slow components. Here, we present a configurable retina simulation environment that accurately reproduces both contrast components. A contrast increase in the visual input accelerates kinetics of the filter, reduces sensitivity and depolarizes the membrane potential. Slow adaptation does not affect the temporal response but produces a progressive hyperpolarization of membrane potential. The implemented model for contrast adaptation provides a neural basis of each retinal stage, from photoreceptors up to ganglion cells, to explain the observed retina behavior. Both forms of contrast adaptation, fast and slow, are captured by a combined model of shunting feedback of bipolar cells and short-term plasticity (STP) at the bipolar-to-ganglion synapse. Biological accuracy of the model is evaluated by comparison of the measured neural response with the simulated response fitted to published physiological data. One problem with the simulated model is finding its optimal parameter settings, since the model response is described by a complex system of different retina stages with linear, nonlinear and feedback connections. We propose to use a multiobjective genetic optimization to automatically search the parameter space and easily find a feasible configuration solution.

Keywords: Visual adaptation · Multiobjective genetic optimization · Retina simulator · Shunting inhibition · Short-term plasticity

1 Introduction

The visual system quickly adapts its dynamic range to encode more efficiently changes in the environment [1–3]. Neural sensitivity is increased when input signals are weak to improve the signal-to-noise ratio. However, when input signals are strong the neural amplification factor is reduced and the time course accelerated to prevent the response from saturation and to anticipate faster temporal patterns. At the earliest stages of the visual system neurons adapt primarily to

I. Rojas et al. (Eds.): IWANN 2015, Part II, LNCS 9095, pp. 175–184, 2015.
DOI: 10.1007/978-3-319-19222-2_15

the mean light intensity and its standard deviation relative to the mean over time, known as temporal contrast. Our work focused on reproducing contrast adaptation mechanisms using a retina model automatically configured by a multiobjective genetic algorithm.

Two different temporal components have been observed for contrast adaptation: a fast change that occurs within the first 100 ms and a slow change over 10 s [4–8]. When contrast of the visual input changes from low to high values, temporal filtering quickly accelerates, sensitivity decreases, and the average response increases. If a high variance is maintained over time, the temporal response is not modified but the ganglion membrane potential shows a slow decay. Upon a decrease in contrast, all these changes reverse direction but with asymmetric time constants for slow adaptation [4,7,9].

Several models have been proposed for contrast adaptation [4,10–13]. However they focused on only a few aspects of adaptation or do not fully characterize all neural stages in the retina. Moreover, some of them used functional modules that do not clearly connect with the underlying biophysical mechanisms. We present a retina model that reproduces both slow and fast components of contrast adaptation and provides a neural mechanism at each retinal stage, from photoreceptors up to ganglion cells, to explain the observed retina behavior. To evaluate the biological accuracy of the model, the physiological experiment described by Ozuysal and Baccus [4] was reproduced using a configurable retina simulation environment that can approximate different retina models. Further details of this platform are provided in previous publications [14]. A multiobjective genetic algorithm automatically fits responses of the simulated multistage model to neural responses measured in the experiment. Since the simulated response and its objective function cannot be easily described by a mathematical model, because of the multiple complex interactions among the different retina stages (e.g., feedback connections), a genetic algorithm is used as an efficient approach to find an optimal solution.

The rest of the paper is organized as follows. In section 2 we detail the neural model implemented to reproduce contrast adaptation. Parameter fitting and simulation results of the physiological experiment are described in section 3. Finally, in section 4, we discuss the conclusions.

2 Retinal Circuitry for Contrast Adaptation

Contrast adaptation originates in bipolar cells and neither photoreceptors nor horizontal cells are involved in the process [5,6]. Recent experiments have shown that contrast adaptation effects are still present under physiological blockade of amacrine synapses, ruling out a critical role for amacrine cells in driving contrast adaptation [2,5,15]. Slow adaptation mechanisms are apparently driven by prolonged depression of glutamate release at bipolar cell synapses [4,9,16–19], whereas inactivation of voltage-dependent Na+ channels in ganglion cells [7,20] and calcium-related mechanism in bipolar cells [15] may be responsible for the fast component. In addition, a large fraction of adaptation has been observed at the bipolar-to-ganglion synapse [5,21].

A well-known mathematical tool, the linear-nonlinear analysis (LN) [5–8,22], is usually used to fully characterize contrast adaptation. A LN analysis generates two output plots, represented by a linear filter and a static nonlinearity, that describe the filtering properties of a neuron. The LN analysis separates the temporal behavior of the cell from nonlinear response components (e.g., synaptic rectification or membrane depolarization). The neural response is first correlated with the input pattern to obtain the temporal filter. This filter is convolved afterwards with the stimulus to generate a linear model of the response. Then, the fixed nonlinearity is calculated by plotting the response against this linear model of the response [2,6].

Our model of contrast adaptation places temporal adaptation and changes of the static nonlinearity at different retina stages. Both forms of contrast adaptation, fast and slow, are captured by a combined model of shunting feedback [10,11] and short-term plasticity (STP) at the bipolar-to-ganglion synapse [4,9,16–19] (Figure 1). A whole retina architecture is described by this model. Every retinal layer of the model is represented by a series of biophysical mechanisms that explain some specific aspect of the signal processing, such as membrane potential integration or synaptic rectification. These mechanisms, provided by a simulation environment [14], are based on well-known retina models recurrently used in the literature to characterize different physiological experiments.

Visual input is first processed by the photoreceptor layer through a double-stage process that includes a temporal linear filter and a static nonlinearity. Since contrast adaptation is not present at this retina stage, a linear approximation of the neural response, $L(t)$, is defined based on the linear kernel $K(x, y, \tau)$ [23,24]:

$$L(t) = \int_0^\infty \mathrm{d}\tau \int_{(x,y)\epsilon RF} K(x, y, \tau) s(x_0 - x, y_0 - y, t - \tau) \mathrm{d}x\mathrm{d}y \tag{1}$$

where $s(x, y, t)$ is the visual stimulus and RF the receptive field of the cell. The neural response depends linearly on all past values of the input stimulus located in the cells receptive field RF. This integral corresponds to the well-defined convolution operation:

$$L(t) = (s * K)(x_0, y_0, t) \tag{2}$$

$K(x, y, t)$ can be broken down as a product of two functions, one that accounts for the spatial receptive field and the other one for the temporal receptive field:

$$K(x, y, t) = K_s(x, y) K_t(t) \tag{3}$$

The spatial receptive field, $K_s(x, y)$, is modeled as a Gaussian function, similarly to kernels used in the receptive field model proposed by Rodieck [25] and Enroth-Cugell and Robson [26]. An exponential cascade function, $E_t(t)$, based on the implementation of Virtual Retina [10], was adapted to model the temporal filter, $K_t(t)$. This type of filters, with multiple low-pass stages, has been commonly used to characterize processes such as the phototransduction cascade in cones [27].

$$E_t(t) = \frac{(nt)^n \exp(-nt/\tau)}{(n-1)!\tau^{n+1}} \tag{4}$$

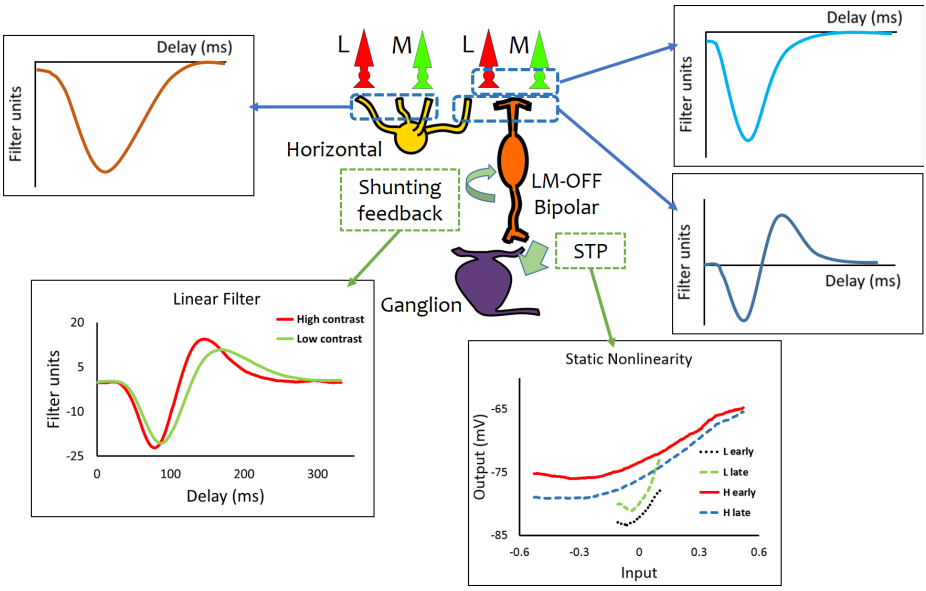

Fig. 1. Schematic view of the retina circuit proposed to reproduce contrast adaptation, where L and M correspond to L- and M-cones, respectively. Temporal kernels of photoreceptors (top-right) and horizontal cells (top-left) are represented by low-pass kernels implemented as exponential cascade filters with different time constants. Subtraction of the signal from photoreceptors and horizontal cells at the Outer Plexiform Layer, which is the layer of neural synapses that connects photoreceptors, horizontal and bipolar cells, produces the typical biphasic shape observed in bipolar and subsequent neural layers. The proposed model places temporal adaptation and changes of the static nonlinearity at different retina stages. Bipolar shunting feedback mechanism is responsible for adaptation of the linear filter, whereas the STP module at bipolar-to-ganglion synapse for polarization and hyperpolarization offsets of the nonlinearity. It is shown at the bottom of the figure a representation of the type of results that are obtained for the contrast experiment (shunting feedback and STP module). Further details of this experiment and the nomenclature used are included in the text and in Figure 2.

The exponential cascade filter peaks at time τ and the filter shape is controlled by the number of low-pass stages, n. The synaptic output of photoreceptors is again delayed by a similar low-pass scheme implemented at horizontal cells (Figure 1). Linear subtraction of the signal from photoreceptors and horizontal cells at the Outer Plexiform Layer, which is the layer of neural synapses that connects photoreceptors, horizontal and bipolar cells, produces the typical biphasic shape observed in bipolar and subsequent neural layers [5,6] (Figure 1).

Membrane potential of bipolar cells is described by a single-compartment model. The basic equation that explains the temporal evolution of a single-compartment model is [23]:

$$C_m \frac{dV(t)}{dt} = \sum_i I_i(t) + \sum_j g_j(E_j(t) - V(t)) \tag{5}$$

where the index j indicates the input ionic channel, C_m is the membrane capacitance, V the membrane potential, g_j is the conductance of the channel, E_j the reversal potential of the channel and the term $\sum_i I_i$ denotes the sum of external input currents. Channel conductances are modified by delayed and rectified feedback from bipolar output to reproduce the shunting inhibition effect. Shunting inhibition has been used to reproduce nonlinear mechanisms of the retina, such as contrast and luminance gain control [10,11], directional selectivity to motion [28,29], and normalization of the linear response in the primary visual cortex [30]. Temporal adaptations in the linear filter of the LN analysis are produced by shunting inhibition (Figure 1).

Polarization and hyperpolarization offsets of the nonlinearity are implemented by a model of short-term plasticity. It was suggested that opposing mechanisms of plasticity (i.e., depression and facilitation) could be combined together to compensate the mutual information loss [31]. Following this idea, the model includes a short-term plasticity module that correlates synaptic weight with the neural input to simulate a depolarizing offset of the ganglion membrane for high contrast steps [4,6]. On the other hand, synaptic depression occurs for maintained values of contrast with the synaptic offset decaying exponentially back to its resting value. This module is defined by:

$$P = P + k_f(k_m(t)abs(input) - P) \tag{6}$$

where P is the offset of the synapse, the parameter k_f controls the degree of facilitation, and the factor $(k_m(t)abs(input) - P)$ prevents the offset from growing indefinitely. A rectification of the input is applied by the term of absolute value. A normalization of the input would be required, and the term would become $abs(input - E_V)$, if the bipolar input had an offset E_V. The variable k_m is responsible for the slow depression of the synapse. Its exponential decay is approximated by:

$$k_m(t+1) = k_{mInf} + (k_m(t) - k_{mInf}) \exp(-step/tau) \tag{7}$$

with a temporal constant defined by the quotient of the simulation *step* and the parameter *tau*. k_{mInf} fixes the resting value and is inversely proportional to the input using a depression factor k_d:

$$k_{mInf} = \frac{k_d}{abs(input)} \tag{8}$$

3 Parameter Fitting and Simulated Neural Response

The model for contrast adaptation is described by a complex multistage system with different retinal layers interconnected by linear, nonlinear and feedback synaptic mechanisms. Thus, its simulated neural response and consequently the optimization error function, understood as the difference between the simulated and the measured responses, cannot be easily described by mathematical functions. Moreover, the lack of smoothness in the error function and the existence of multiple local minima are another critical aspects to be considered when selecting the optimization method. A multiobjective genetic algorithm can be an efficient and easy solution to simultaneously fit the model to the different measured neural responses.

We fit the model using a multiobjective genetic algorithm provided by the Python library DEAP [32]. DEAP is a very flexible and intuitive evolutionary computation framework that allows a rapid prototyping of different optimization algorithms. Besides, the retina simulation platform is interfaced with NEST [33] to generate spiking activity of ganglion cells. An evolutionary computation tool that is executed in Python, such as DEAP, facilitates its integration with the NEST simulation script, defined in PyNEST (its Python interface), and simplifies the code by combining both simulation and optimization into a single script.

A general evolutionary search was configured whereby the random initial population of solutions is evolved by applying crossover (two-point crossover)

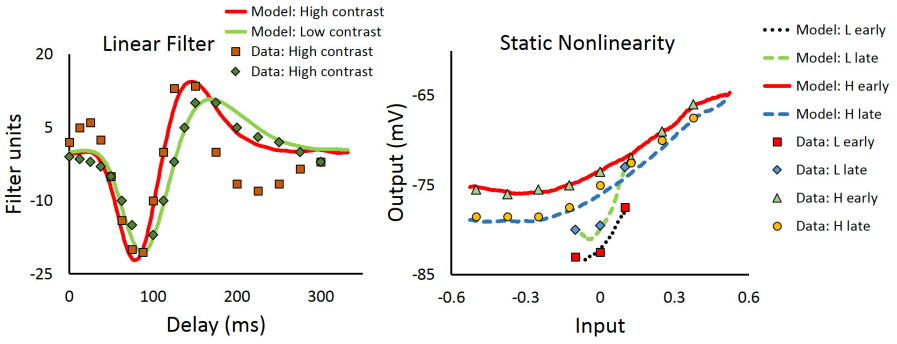

Fig. 2. Comparison of the LN analysis obtained from simulation results (solid line) and the LN analysis of physiological data (markers). Four different contrast intervals are considered in the measurements: 'L early' corresponds to the first 10 seconds after a low contrast step and 'L late' to the period from 10 to 20 seconds after a low contrast step. 'H early' and 'H late' are defined similarly for a high contrast step. A contrast increase in the visual input accelerates kinetics of the filter and its response becomes more differentiating. At the same time, the static nonlinearity shows an increase of the offset and a decrease of the average slope. Slow adaptation does not affect the temporal response, thus only two contrast periods are considered for the linear filter, but produces a progressive hyperpolarization of membrane potential.

and mutation (gaussian mutation) operators in combination with a selection mechanism (tournament selection). Individuals are evaluated every new generation by a multiobjective fitness function with the same minimization weights for all objectives. The fitness function simulates a forty-second sequence of the retina model with parameters set by values of the individual evaluated. It computes then the LN analysis of simulation results and generates an error metric between simulated and measured data. By simplicity and effectiveness, a mean squared error (MSE) was used as estimator of this error function:

$$MSE = \sum_i (r_{measured}(i) - r_{simulated}(i))^2 \tag{9}$$

where $r_{measured}$ are sampled values from the LN analysis of physiological results and $r_{simulated}$ are generated by simulation. Target physiological data were obtained by sampling curves of the LN analysis published by Ozuysal and Baccus [4]. Nearly total independence of the shunting feedback mechanism, affecting only the linear filter, and the STP module, responsible for variations of the offset, allows a double-stage minimization process that reduces the parameter search space and hence the computation time.

Twelve parameters of the retina model, up to bipolar cells, were first fitted simultaneously to the high and low contrast curves of the linear filter. These parameters control the shape of temporal kernels, such as τ and n in equation 4,

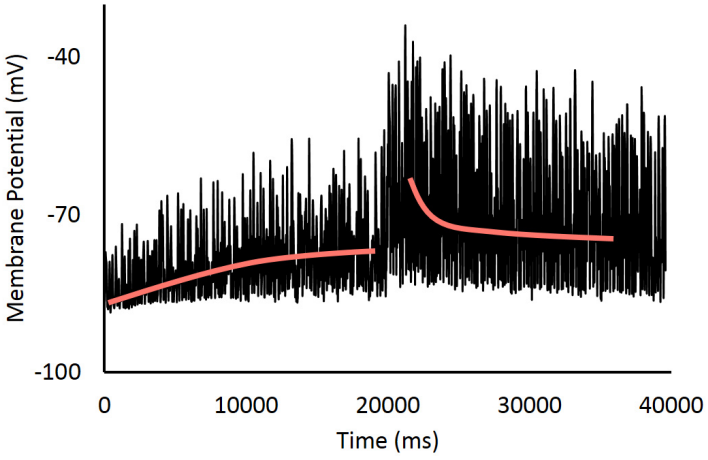

Fig. 3. Simulated neural response of ganglion cells over time. A low contrast stimulus is presented from 0 to 20000 ms, after a high contrast period before 0 ms. At 20000 ms there is a high contrast step. The response to a high contrast step is characterized by two distinctive temporal behaviors: first a fast hyperpolarization of the membrane potential is produced, followed by a slow decay with a higher time constant. A low contrast step is described by a single time constant that produces a slow increase in the offset, prolonged over the whole period.

and the shunting feedback mechanism described in equation 5. Then, by fixing the optimized parameters of the first retina stages we fitted seven parameters of the STP module to the four curves observed for the static nonlinearity (Figure 2). Optimal parameter values are within the biological range reported in different physiological studies (e.g., values of τ for photoreceptors and the slow mechanism of the STP module are 0.085 and 12 s, respectively).

For a high step contrast, the retina model captures both the decrease in the time to peak and a more differentiating response of the linear filter, and the decrease of the average slope of the nonlinearity. Similarly to the LNK model [4] our simulation cannot reproduce oscillations of the high contrast curve at the beginning (< 50 ms) and the end (> 150 ms) of the filter time course. These oscillations of the high contrast curve do not represent the neural response of all cells measured [6,21]. However, they tend to appear in cells that strongly adapt to contrast and further research is required to model this behavior.

A high contrast step also produces a fast depolarization of the membrane that is represented by the increase of the offset in the static nonlinearity (Figure 2). When a high variance is maintained over time the temporal response is not modified but the membrane potential shows a slow decay. Upon a decrease in contrast, all these changes reverse direction but with asymmetric time constants for slow adaptation [4,7] (Figure 3).

4 Discussion

We described a neural model that reproduces contrast adaptation in the retina. Both forms of contrast adaptation, fast and slow, are captured by a combined model of shunting feedback [10,11] and short-term plasticity at the bipolar-to-ganglion synapse [4,9,16–19] (Figure 1). Unlike other models, a whole retina architecture is proposed, which provides a neural basis of each retinal stage, from photoreceptors up to ganglion cells, to explain the observed retina behavior. We used the neural modules provided by a simulation environment [14] that reproduce widely studied properties of the retina processing, such as membrane potential integration or synaptic rectification.

We fit the model using a multiobjective genetic approach since it provides an easy an efficient solution for dealing with the complexity of the simulated response and its objective function. Target physiological data were obtained by the LN analysis published by Ozuysal and Baccus [4]. Independence of the shunting feedback mechanism, affecting only the linear filter, and the STP module, responsible for variations of the offset, allows a double-stage minimization process that reduces the computational load of searching the whole parameter space. However, we think that a one-step minimization process may improve the fitting of some intervals, such as the oscillations observed in some parts of the high contrast curve. Another computation architectures should be then studied (e.g., high-performance computing) to speed up the optimization process. Different optimization strategies can be also considered to fully exploit the potential of this model.

Acknowledgments. This work has been supported by the Human Brain Project (SP11 - Future Neuroscience), project P11-TIC-7983, Junta of Andalucia (Spain), Spanish National Grant TIN2012-32039, co-financed by the European Regional Development Fund (ERDF), and the Spanish Government PhD scholarship FPU13/01487.

References

1. Rieke, F., Rudd, M.E.: The challenges natural images pose for visual adaptation. Neuron **64**(5), 605–616 (2009)
2. Demb, J.B.: Functional circuitry of visual adaptation in the retina. The Journal of Physiology **586**(18), 4377–4384 (2008)
3. Kohn, A.: Visual adaptation: physiology, mechanisms, and functional benefits. Journal of Neurophysiology **97**(5), 3155–3164 (2007)
4. Ozuysal, Y., Baccus, S.A.: Linking the computational structure of variance adaptation to biophysical mechanisms. Neuron **73**(5), 1002–1015 (2012)
5. Beaudoin, D.L., Borghuis, B.G., Demb, J.B.: Cellular basis for contrast gain control over the receptive field center of mammalian retinal ganglion cells. The Journal of Neuroscience **27**(10), 2636–2645 (2007)
6. Baccus, S.A., Meister, M.: Fast and slow contrast adaptation in retinal circuitry. Neuron **36**(5), 909–919 (2002)
7. Kim, K.J., Rieke, F.: Temporal contrast adaptation in the input and output signals of salamander retinal ganglion cells. The Journal of Neuroscience **21**(1), 287–299 (2001)
8. Chander, D., Chichilnisky, E.: Adaptation to temporal contrast in primate and salamander retina. The Journal of Neuroscience **21**(24), 9904–9916 (2001)
9. Manookin, M.B., Demb, J.B.: Presynaptic mechanism for slow contrast adaptation in mammalian retinal ganglion cells. Neuron **50**(3), 453–464 (2006)
10. Wohrer, A., Kornprobst, P.: Virtual retina: a biological retina model and simulator, with contrast gain control. Journal of Computational Neuroscience **26**(2), 219–249 (2009)
11. Mante, V., Bonin, V., Carandini, M.: Functional mechanisms shaping lateral geniculate responses to artificial and natural stimuli. Neuron **58**(4), 625–638 (2008)
12. van Hateren, J.V., Rüttiger, L., Sun, H., Lee, B.: Processing of natural temporal stimuli by macaque retinal ganglion cells. The Journal of Neuroscience **22**(22), 9945–9960 (2002)
13. Victor, J.D.: The dynamics of the cat retinal x cell centre. The Journal of Physiology **386**(1), 219–246 (1987)
14. Martínez-Cañada, P., Morillas, C., Nieves, J.L., Pino, B., Pelayo, F.: First stage of a human visual system simulator: the retina. In: Trémeau, A., Schettini, R., Tominaga, S. (eds.) CCIW 2015. LNCS, vol. 9016, pp. 118–127. Springer, Heidelberg (2015)
15. Rieke, F.: Temporal contrast adaptation in salamander bipolar cells. The Journal of Neuroscience **21**(23), 9445–9454 (2001)
16. Euler, T., Haverkamp, S., Schubert, T., Baden, T.: Retinal bipolar cells: elementary building blocks of vision. Nature Reviews Neuroscience **15**(8), 507–519 (2014)
17. Jarsky, T., Cembrowski, M., Logan, S.M., Kath, W.L., Riecke, H., Demb, J.B., Singer, J.H.: A synaptic mechanism for retinal adaptation to luminance and contrast. The Journal of Neuroscience **31**(30), 11003–11015 (2011)
18. Dunn, F.A., Rieke, F.: Single-photon absorptions evoke synaptic depression in the retina to extend the operational range of rod vision. Neuron **57**(6), 894–904 (2008)

19. Singer, J.H., Diamond, J.S.: Vesicle depletion and synaptic depression at a mammalian ribbon synapse. Journal of Neurophysiology **95**(5), 3191–3198 (2006)
20. Kim, K.J., Rieke, F.: Slow na+ inactivation and variance adaptation in salamander retinal ganglion cells. The Journal of Neuroscience **23**(4), 1506–1516 (2003)
21. Zaghloul, K.A., Boahen, K., Demb, J.B.: Contrast adaptation in subthreshold and spiking responses of mammalian y-type retinal ganglion cells. The Journal of Neuroscience **25**(4), 860–868 (2005)
22. Zaghloul, K.A., Boahen, K., Demb, J.B.: Different circuits for on and off retinal ganglion cells cause different contrast sensitivities. The Journal of Neuroscience **23**(7), 2645–2654 (2003)
23. Dayan, P., Abbott, L.: Theoretical neuroscience: computational and mathematical modeling of neural systems. Journal of Cognitive Neuroscience **15**(1), 154–155 (2003)
24. Wohrer, A.: Model and large-scale simulator of a biological retina, with contrast gain control. PhD thesis, Nice (2008)
25. Rodieck, R.W.: Quantitative analysis of cat retinal ganglion cell response to visual stimuli. Vision Research **5**(12), 583–601 (1965)
26. Enroth-Cugell, C., Robson, J.G.: The contrast sensitivity of retinal ganglion cells of the cat. The Journal of Physiology **187**(3), 517–552 (1966)
27. Smith, V.C., Pokorny, J., Lee, B.B., Dacey, D.M.: Primate horizontal cell dynamics: an analysis of sensitivity regulation in the outer retina. Journal of Neurophysiology **85**(2), 545–558 (2001)
28. Torre, V., Poggio, T.: A synaptic mechanism possibly underlying directional selectivity to motion. Proceedings of the Royal Society of London. Series B. Biological Sciences **202**(1148), 409–416 (1978)
29. Amthor, F.R., Grzywacz, N.M.: Nonlinearity of the inhibition underlying retinal directional selectivity. Visual Neuroscience **6**(03), 197–206 (1991)
30. Carandini, M., Heeger, D.J., Movshon, J.A.: Linearity and normalization in simple cells of the macaque primary visual cortex. The Journal of Neuroscience **17**(21), 8621–8644 (1997)
31. Kastner, D.B., Baccus, S.A.: Coordinated dynamic encoding in the retina using opposing forms of plasticity. Nature Neuroscience **14**(10), 1317–1322 (2011)
32. Fortin, F.-A., De Rainville, F.-M., Gardner, M.-A., Parizeau, M., Gagné, C.: DEAP: Evolutionary algorithms made easy. Journal of Machine Learning Research **13**, 2171–2175 (2012)
33. Gewaltig, M.-O., Diesmann, M.: Nest (neural simulation tool). Scholarpedia **2**(4), 1430 (2007)